



Petrochemical studies of metapelites of the area around Sonapahar, Meghalaya, India

V. Vanthangliana^{*1}, M. F. Hussain² and Jimmy Lalnunmawia¹

¹ Department of Geology, Mizoram University, Aizawl 796009, India

² Department of Earth Sciences, Assam University, Silchar 788011, India

Received 22 November 2010 | Revised 25 February 2011 | Accepted 1 March 2011

ABSTRACT

Metapelites form a dominant component of the Precambrian basement complex in the Sonapahar area of Shillong Plateau, north-east India. In this paper, a new data on the major, minor and trace element compositions of these metapelites, an important member of the Precambrian basement rocks found in the Shillong plateau is reported. Petro-chemical data on these rocks were used to reproduce the nature and composition of their protolith. The mineral assemblages and petrographical observations indicated that metapelites of the study area were metamorphosed up to amphibolite to granulite facies metamorphism. Chemically, metapelites are characterized by relatively high Al₂O₃ (11.35-19.91 wt%), enrichments in MgO, FeO, MnO and TiO₂; depletions in Na₂O and especially CaO; low concentrations of Sc, Cr, Co, Ni, and Sr; high concentrations of Y, Nb, Zr, Hf, Ta, Th, U, and REE (rare earth elements) with prominent negative Eu-anomalies. Results indicated that these rocks were redeposited and metamorphosed products of Precambrian weathering crusts. The protolith of the metapelites was produced by erosion products of acid rocks, which were which are emplaced in volcanic arc environment.

Key words: Geochemistry; metapelites; petrography; Shillong Plateau; Sonapahar.

INTRODUCTION

Precambrian basement of the Shillong plateau is made up of high grade gneisses which are intruded by basic and ultrabasic rocks of different ages. In Sonapahar area, metapelites were largely exposed and occurred intimately associated with granite gneisses and basic

granulites (Fig. 1). Very little work has been conducted on these metapelites and there are not enough data to understand the nature and evolutionary history of these rocks as it is an important indicators of the composition of the continental crust. Earlier workers were mostly petrological accounts, however, detail description of metamorphic rocks the area around Sonapahar base on geochemical data is still very limited.

The Shillong Plateau, elsewhere considered a detached Precambrian block of Indian

Corresponding author: Vanthangliana
Phone: +91-9862501966
E-mail: vantea_g@yahoo.com

Peninsula in the northeast India is bounded to the south east by E-W trending Dauki fault (Fig. 2), to the north by Brahmaputra fault¹ or Oldham fault,² to the west by the broadly NNE-SSW Indo-Myanmar belt. The plateau is separated from Mikir Hills in the Northeast by the alluvium tract of the Kopili fault system.³ The demonstrable recognition of Mesoproterozoic granulites in the Shillong Meghalaya Gneissic Complex (SMGC) is new and their similarity with temporally related rocks elsewhere in the Indian shield indicates that the Shillong Plateau has been a part of the Indian shield since the Mesoproterozoic. It is suggested that the Pan-African suture passing through Prydz Bay in Antarctica possibly continued northward into India through the SMGC with the western margin of the suture between the Sonapahar and the Garo-Goalpara Hills regions.⁴ The geology of the Shillong plateau is very complex, as the plateau represents a checkered history of evolution with contrasting petrological units of different ages, consisting of gneisses, metasedimentary supracrustals, granitoids, mafic dykes, alkaline and carbonate rocks and Trap rocks. Rocks of upper amphibolite to granulite facies, flanked on the east by greenschists facies rocks belonging to the Shillong Series of Precambrian age and to the south by sedimentary rocks and basic volcanics of cretaceous age are present.⁵ The area is dominated by blastoporphyratic granite and granite gneisses intrusive into the basement gneisses. Cordierite-garnet-biotite-sillimanite gneisses interlayered with quartz-sillimanite schists, non-garnetiferous mafic granulites and rare calc silicate gneisses occur as distended bands and lenses within the granites.⁵

Composition of rocks and their source rocks are efficiently studied by analysis of the major oxides, REE concentrations and other trace elements; because trace elements, including REE, are weakly fractionated in the processes of sedimentation and metamorphism, so that the rocks even when metamorphosed to high pressures of the granulite fa-

cies retain their geochemical signatures inherited from the source rocks.⁶ It is reasonable to believe that shales and the products of their metamorphism are indicators of the composition of the continental crust in terms of the behavior of trace elements and the geochemical record of these rocks makes it possible to trace the evolution of this crust.⁷ This study is an attempt to throw light on the petrochemical characters and nature of protolith of metapelites base on a major and trace element including REE which constitute the major metamorphic rock types of the area.

MATERIALS AND METHODS

For microscopic studies, thin sections were prepared at the Department of Geology, Kumaun University, Nainital, and preparation for some slides and detailed petrographic studies were done at the Department of Geology, Mizoram University, using Leica DMEP trinocular model. For geochemical analysis, samples were pulverized using an agate mortar at NGRI, Hyderabad. Major elements were analysed by XRF (Philips MagiX PRO PW 2440 wavelength dispersive X-ray fluorescence spectrometer with automatic sample changer PW 2540).

For the dissolution of samples for analysis of Trace element and REE by ICP-MS, a Perkin Elmer SCIEX (ELAN DRC II ICP-mass spectrometer, Toronto, Canada) was used. During analysis, natural standards viz. JG-2, AG-2 and SDC-1 were also analyzed simultaneously to check the precision and accuracy of analytical data. The procedures followed in the preparation of the rock samples for analyses on XRF and ICP-MS were of national and international standards.^{8,9}

RESULTS AND DISCUSSIONS

Petrography

Of the rock types of the study area, the study was concentrated on cordierite bearing

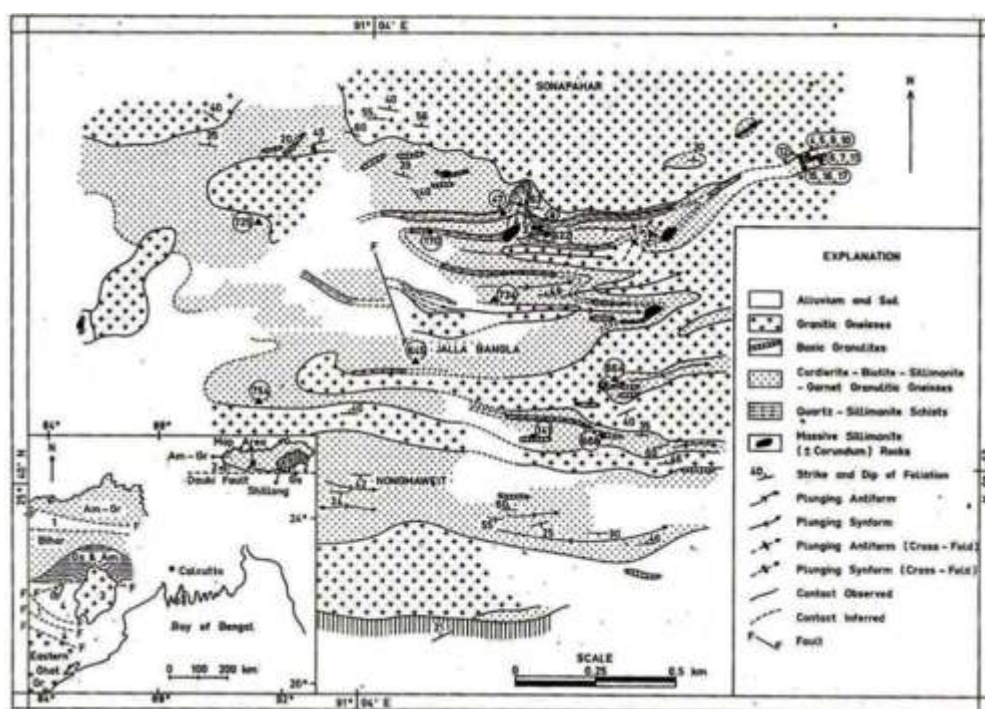


Figure 1. Geological map of the area around Sonapahar, Meghalaya.

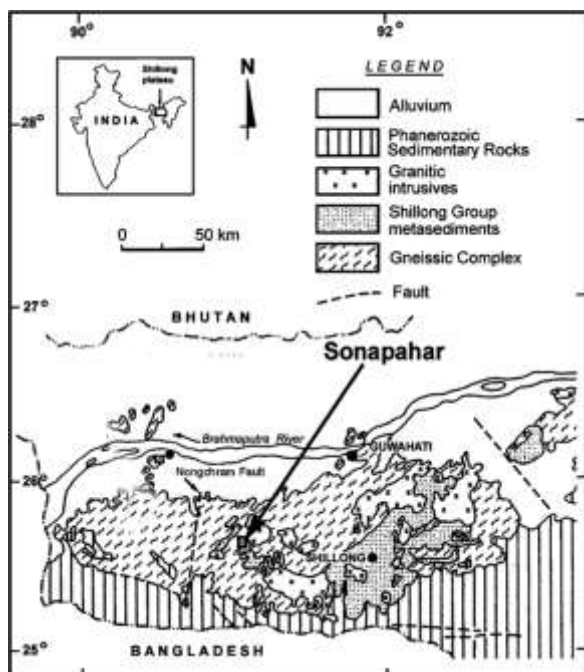


Figure 2. Generalized geological map of the Shillong-Meghalaya Gneissic

granulitic gneisses (referred to as metapelites in this study). Metapelites were medium to fine grained with gneissose structure having garnet as one of their constituent minerals. Some samples were massive and the foliation cannot be identified. In places, porphyroblast cordierites were clearly visible in hand specimen (Fig. 3). The rocks were melanocratic. Dark colored is mainly imparted by the presence of biotite. The foliation was well defined by parallel orientation of biotite flakes. Other identified minerals in hand specimen were sillimanite and quartz.

Under microscope, metapelites were characterized by a medium to fine grained mosaic of equant, polyonal, strain free grains of mesoperthitic K-felspar (Kf), cordierite (Cd), biotite (Bt), sillimanite (Sill), plagioclase (Plag) and garnet (Gt). The dominant fabric (S_2) is defined by quartz ribbons and preferred alignment of biotite and to a lesser extent of sillimanite.

Garnet occurred as coarse xenoblasts and

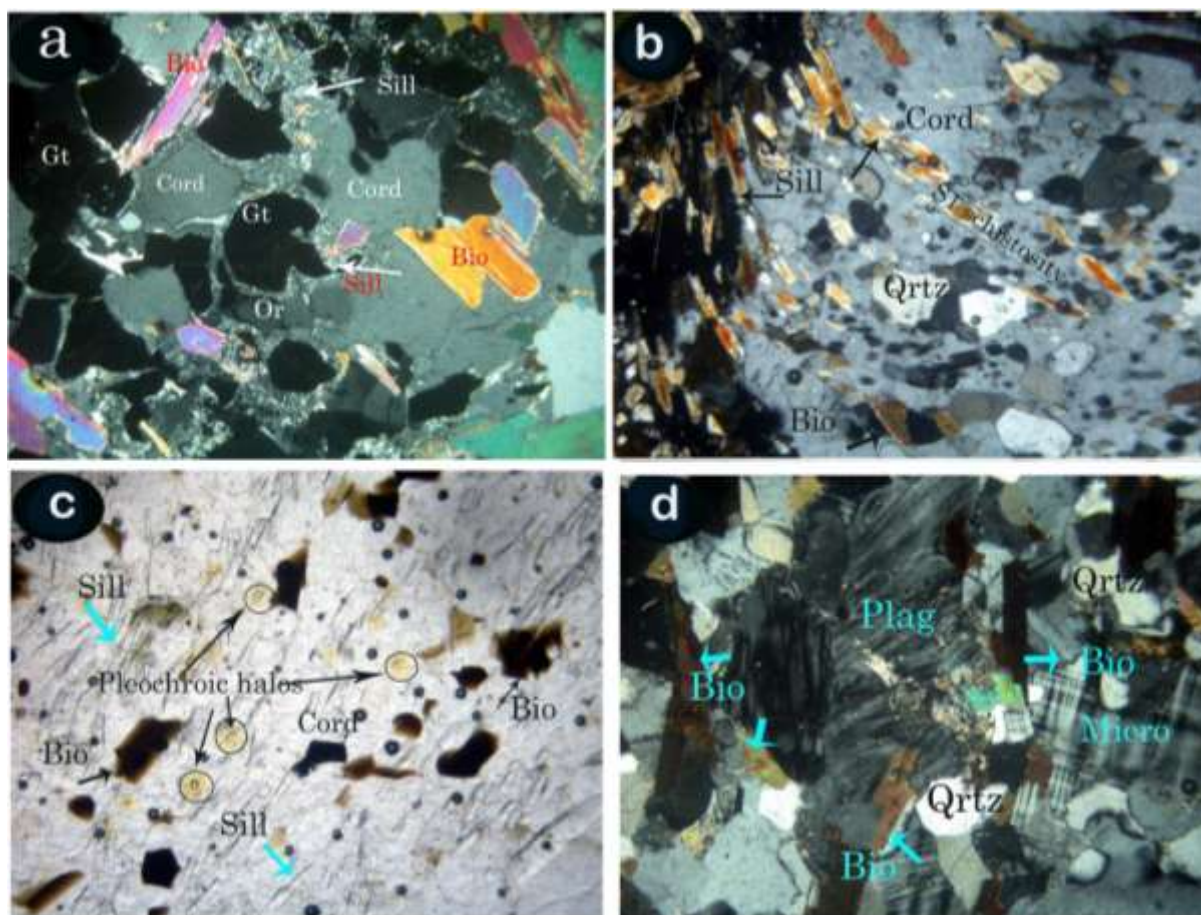
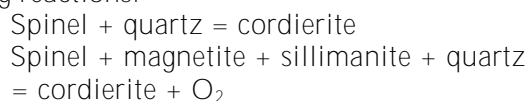


Figure 3. Photomicrograph of metapelites. a) Fibrous sillimanite (Sill) occur at garnet grain boundaries replacing garnet at grain edges within cordierite (under cross polarized light). b) Porphyroblast cordierite (Cord) crystal with numerous inclusions of needle sillimanite, quartz and biotite (Bio) (under cross polarized light). Note that sillimanite inclusion define S_1 schistosity. c) Cordierite (Cord) porphyroblast showing pleochroic halos (under plane polarized light). d) Strain plagioclase (Plag) crystal which was partly sericitized (under cross polarized light.)

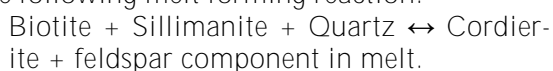
is poikiloblastic containing biotite. The grains were devoid of rational faces (Fig. 3a). At places, garnet grains appeared to be replaced by the intergrowth of biotite and plagioclase. Inclusions of sillimanite, biotite and K-Felspar in garnet were common. However, cordierite was never included in garnet. The external schistosity (S_2) did not demonstrably wrap around, but neither did the schistosity passed through the garnet grains. It is likely

that garnet formed prior to the S_2 schistosity. In some slides, garnet were highly fractured and partially rimmed by sillimanite, biotite and cordierite. Cordierite occurred as coarse xenoblasts crystal or in coarse granular aggregates which overprint the fabric of the matrix. Some cordierite grains showed characteristic pleochroic halos (Fig. 3c). Inclusion of quartz with rounded shapes and of biotite in a large grain of cordierite was commonly observed.

The inclusion showed evidence of adjustment of their boundaries towards low energy configurations. In some cases, aggregates of S_2 biotite grains weakly wrapped around the cordierite grains, but cordierite hosted inclusion trails (S_1) biotite-sillimanite defined foliation (Fig. 3b). These textural relations suggest biotite + sillimanite recrystallization broadly syn-tectonic with respect to the S_2 fabric. Occasionally, the cordierite grains contained inclusions of quartz and spinel. This textural relation may be explained by the cordierite forming reactions:



At places, cordierite was wrapped by needles of sillimanite and flakes of biotite. Inclusion of sillimanite, biotite, quartz and magnetite was commonly seen within cordierite. The ubiquitous presence of coarse poikiloblasts of cordierite with numerous inclusions of sillimanite, biotite and quartz (Fig. 2e) suggests the following melt forming reaction:



Sillimanite occurred as coarse prismatic crystals and sometimes fibrous, usually colorless. Both textural type of sillimanite define the S_2 fabric. In places, fibrolite occurred at garnet grain boundaries replacing garnet at grain edges (Fig. 3a). In some samples, fibrous sillimanite were enveloped by growth of cordierite grains and occurred as inclusion but still defining S_2 fabric.

Biotite commonly occurred as small flakes. Biotite are oriented parallel to foliation and the alignment defined the dominant fabric S_2 . Two generation of biotite was identified, primary biotite that exists before garnet mostly occurred as inclusion in the latter. Secondary biotite defines S_2 fabric. Both microcline and orthoclase were present, but orthoclase was less common and mostly occurred as medium grained. Inclusion of some opaque minerals, biotite, quartz, and apatite were present. K-Feldspar also showed undulose extinction sug-

gesting post crystalline deformation. Plagioclase was less dominant in comparison to K-feldspar. Strained plagioclases with partly sericitised were occasionally observed (Fig. 3d). They were medium to fine grained, sub-idioblastic to idioblastic. The anorthite content in plagioclase is (An_{30-35}).

Major elements

Metapelites were characterized by SiO_2 (57.42-68.61 wt %), relatively high Al_2O_3 (11.35-.91 wt %), enrichments in MgO (2.23-4.80 wt %) and FeOt (4.29-11.48 wt %), depletions in CaO (0.23-1.12 wt %) except one sample with unusually high CaO content (8.13 wt %). Values of K_2O were greater than Na_2O in average. They were mostly enriched in Al_2O_3 , Fe_2O_3 , FeOt, MgO, MnO and TiO_2 but poor in CaO and K_2O (Table. 1). In Harkers variation diagram, SiO_2 values showed a pronounced inverse correlation with Al_2O_3 , Fe_2O_3 , MnO, MgO and TiO_2 in all the samples (Fig. 4). A poor correlation was observed with CaO, K_2O and Na_2O which may be due to mobilization of K and Na during metamorphism and weathering. Based on the chemical classification,¹⁰ these rock are classed as aluminous [$X_{\text{AL}} = (\text{Al}_2\text{O}_3 - 3\text{K}_2\text{O}) / (\text{Al}_2\text{O}_3 - 3\text{K}_2\text{O} + \text{FeO} + \text{MgO} + \text{MnO})$] = 0.42-0.62 as compared to the average compositions of typical metapelites and PAAS (Post Australian Archean Shale), which have lower $X_{\text{AL}} = 0.13$.

Petrochemical data allowed us to identify their protoliths and to reproduce the environment in which they formed. Some conventionally used petrochemical ratios such as the chemical index of alteration (CIA),¹¹ chemical index of weathering (CIW),¹² Index of compositional variety (ICV),⁶ and the plagioclase of index of alteration (PIA),¹³ has been used for these purpose. High values of CIA (61.6-92.47) except sample 22 which is 49.52, CIW (73.7-98.6) with one sample 52.11, and PIA (67.29-98.51) with one sample 49.46 (Table 2) suggested that pelites were formed from the

Table 1. Representative major chemistry analysis and CIPW norms of metapelites from Sonapahar.

Sample	S08-18	S08-21	S08-22	S08-33	S08-34	S08-37	S08-41	S08-9	S08-16	S08-6	PAAS
SiO ₂	67.59	66.44	57.42	62.82	67.10	65.29	68.69	65.43	65.95	64.04	62.80
Al ₂ O ₃	15.93	16.11	11.35	19.91	15.06	15.69	15.45	16.38	16.01	16.61	1.00
Fe ₂ O ₃	3.74	4.26	6.69	4.10	4.41	2.50	3.17	3.66	3.62	4.78	10.40
FeOt	6.42	7.31	11.48	7.04	7.57	4.30	5.45	6.29	6.22	8.21	17.85
MnO	0.07	0.11	0.18	0.12	0.07	0.07	0.07	0.10	0.08	0.11	7.22
MgO	3.29	3.69	4.13	6.07	3.89	2.23	2.91	3.30	3.42	4.80	0.11
CaO	0.57	1.04	8.13	0.15	0.21	1.12	0.71	0.65	0.96	0.23	2.20
Na ₂ O	0.93	1.80	2.30	0.13	0.47	4.47	1.31	1.45	1.53	0.40	1.30
K ₂ O	2.88	2.76	1.14	1.34	2.82	4.19	2.93	3.55	3.57	2.50	1.20
TiO ₂	0.57	0.60	1.16	0.51	0.66	0.44	0.42	0.52	0.52	0.78	3.70
P ₂ O ₅	0.03	0.03	0.33	0.04	0.03	0.05	0.04	0.05	0.05	0.03	0.16
Total	102.02	104.15	104.31	102.22	102.30	100.35	101.15	101.38	101.94	102.49	107.94
A/CNK	2.80	2.06	0.57	10.3	3.58	1.13	2.34	2.21	1.97	4.39	0.13
CIPW NORM											
Q	47.19	38.99	23.21	50.08	50.05	18.40	46.09	39.16	38.00	47.29	56.69
C	10.79	8.61	0.00	18.98	11.53	1.96	9.33	9.56	8.36	13.68	0.00
Or	17.81	16.84	7.26	8.32	17.59	25.78	18.10	22.06	22.04	15.67	6.06
Ab	8.23	15.73	20.97	1.16	4.20	39.38	11.58	12.90	13.53	3.59	0.00
An	2.75	5.13	18.61	0.51	0.89	5.45	3.41	3.05	4.64	1.00	0.00
Hy(MS)	8.57	9.49	4.25	15.88	10.23	5.78	7.57	8.64	8.90	12.68	0.00
Il	0.16	0.24	0.42	0.27	0.16	0.16	0.16	0.23	0.18	0.25	7.80
Hm	3.91	4.40	7.21	4.31	4.66	2.61	3.32	3.85	3.79	5.07	0.00
Ru	0.51	0.49	0.00	0.39	0.61	0.38	0.36	0.43	0.45	0.70	0.00

Table 2. Weathering indices of representative metapelite samples from Sonapahar.

Sample	S08-18	S08-21	S08-22	S08-33	S08-34	S08-37	S08-41	S08-9	S08-16	S08-6
CIA	78.43	74.21	49.52	92.48	81.14	61.60	75.74	74.35	72.54	84.14
CIW	91.39	85.01	52.11	98.61	95.68	73.73	88.44	88.64	86.54	96.35
PIA	89.69	82.46	49.47	98.52	94.74	67.29	86.11	85.93	83.32	95.73
ICV	0.72	0.81	1.36	0.61	0.81	0.88	0.70	0.76	0.79	0.80

material of weathering crusts redeposit in warmed and humid climate. This conclusion was confirmed by the ICV values (all less than 1), which implies that the eroded material coming to the sedimentation was more geochemically mature.¹⁴

Trace elements

The concentrations of Sc (4.42-9 ppm), Cr (3.57-7.86 ppm), Co (9.52-18.05 ppm) and Ni (1.42-3.80 ppm) are all low. There is no significant correlation with SiO₂ in the metape-

Table 3. Trace and rare earth element compositions of the metapelites (in parts per million) from Sonapahar.

Sample	S08-18	S08-21	S08-22	S08-33	S08-34	S08-37	S08-41	S08-9	S08-16	S08-6	PAAS
Sc	8.11	8.05	9.01	5.65	9.08	6.06	4.42	7.26	7.44	8.26	16.00
V	39.89	41.41	34.51	35.15	41.58	30.32	26.12	38.94	42.44	50.45	150.00
Cr	6.69	6.78	6.73	7.86	5.82	3.58	5.85	7.52	6.24	7.35	110.00
Co	13.67	18.06	12.81	10.71	15.36	9.59	9.53	14.39	13.95	17.69	23.00
Ni	2.21	2.90	2.38	3.80	2.38	1.43	1.46	2.59	2.10	3.79	55.00
Cu	1.60	1.89	1.30	0.23	0.25	0.49	0.22	1.44	1.31	0.27	50.00
Zn	32.83	69.46	44.82	26.98	48.46	29.35	13.63	55.57	30.48	41.12	85.00
Ga	18.06	24.60	20.22	32.05	30.37	22.58	22.72	24.06	23.21	24.44	
Rb	173.61	166.63	224.45	101.75	153.31	175.34	153.88	211.95	200.01	144.27	160.00
Sr	49.98	64.54	94.64	9.32	18.14	89.15	82.71	63.80	79.95	25.35	200.00
Y	16.46	22.32	18.80	29.63	17.37	16.95	27.27	18.66	17.58	20.65	27.00
Zr	23.94	28.78	50.68	45.50	12.46	96.66	31.63	31.52	35.82	12.78	210.00
Nb	10.64	15.03	13.76	8.01	17.15	12.45	10.66	13.61	11.12	12.40	19.00
Cs	7.13	7.06	4.87	5.24	5.06	6.97	6.45	11.26	7.43	5.56	15.00
Ba	358.47	484.94	586.19	156.26	450.38	550.25	505.30	418.70	455.57	505.29	650.00
Hf	0.80	0.93	1.66	1.59	0.45	3.06	0.99	1.07	1.21	0.46	5.00
Ta	0.36	0.63	0.81	0.58	0.60	0.72	0.60	0.97	0.51	0.65	1.50
Th	21.17	31.84	22.47	36.22	24.74	15.76	30.70	20.52	20.32	26.44	14.63
U	2.72	2.02	3.27	4.36	2.49	2.60	3.12	3.05	2.69	2.89	3.10
La	50.27	75.92	56.28	78.76	50.19	46.01	63.24	52.25	52.16	57.95	
Ce	105.54	156.25	117.85	170.23	106.16	91.82	138.47	107.79	106.38	123.68	
Pr	11.22	16.33	12.56	18.31	11.47	9.34	15.26	11.39	11.07	13.12	
Nd	43.46	62.51	48.59	72.42	43.43	36.08	61.50	43.87	43.42	52.33	
Sm	8.07	10.99	9.00	12.96	7.71	6.42	11.76	8.19	7.76	9.53	
Eu	1.05	1.23	1.40	0.67	0.89	1.33	0.94	1.12	1.36	0.95	
Gd	6.29	8.79	7.06	10.17	5.87	5.20	9.37	6.71	6.23	7.52	
Tb	0.85	1.15	0.98	1.40	0.80	0.71	1.32	0.93	0.85	1.03	
Dy	4.16	5.58	4.78	7.01	3.97	3.71	6.67	4.69	4.19	4.95	
Ho	0.34	0.44	0.39	0.61	0.34	0.34	0.55	0.38	0.35	0.42	
Er	0.94	1.16	1.05	1.71	0.95	1.06	1.43	1.00	1.00	1.09	
Tm	0.07	0.09	0.09	0.01	0.09	0.14	0.12	0.10	0.08	0.09	
Yb	0.57	0.67	0.74	1.15	0.72	1.67	0.85	0.94	0.69	0.71	
Lu	0.08	0.10	0.11	0.17	0.12	0.29	0.12	0.16	0.11	0.09	
ΣREE	232.90	341.20	260.87	375.58	232.69	204.12	311.59	239.51	235.65	273.45	
Eu/Eu*	0.44	0.37	0.52	0.17	0.39	0.68	0.27	0.45	0.58	0.33	
(La/Yb) _N	62.82	81.65	54.40	48.95	49.87	19.73	53.24	39.78	54.16	58.30	
K/Rb	137.73	137.52	42.17	109.34	152.72	198.40	158.09	139.06	148.19	143.87	
Th/U	7.79	15.76	6.88	8.31	9.92	6.06	9.85	6.73	7.56	9.16	
La/Th	2.38	2.38	2.50	2.17	2.03	2.92	2.06	2.55	2.57	2.19	

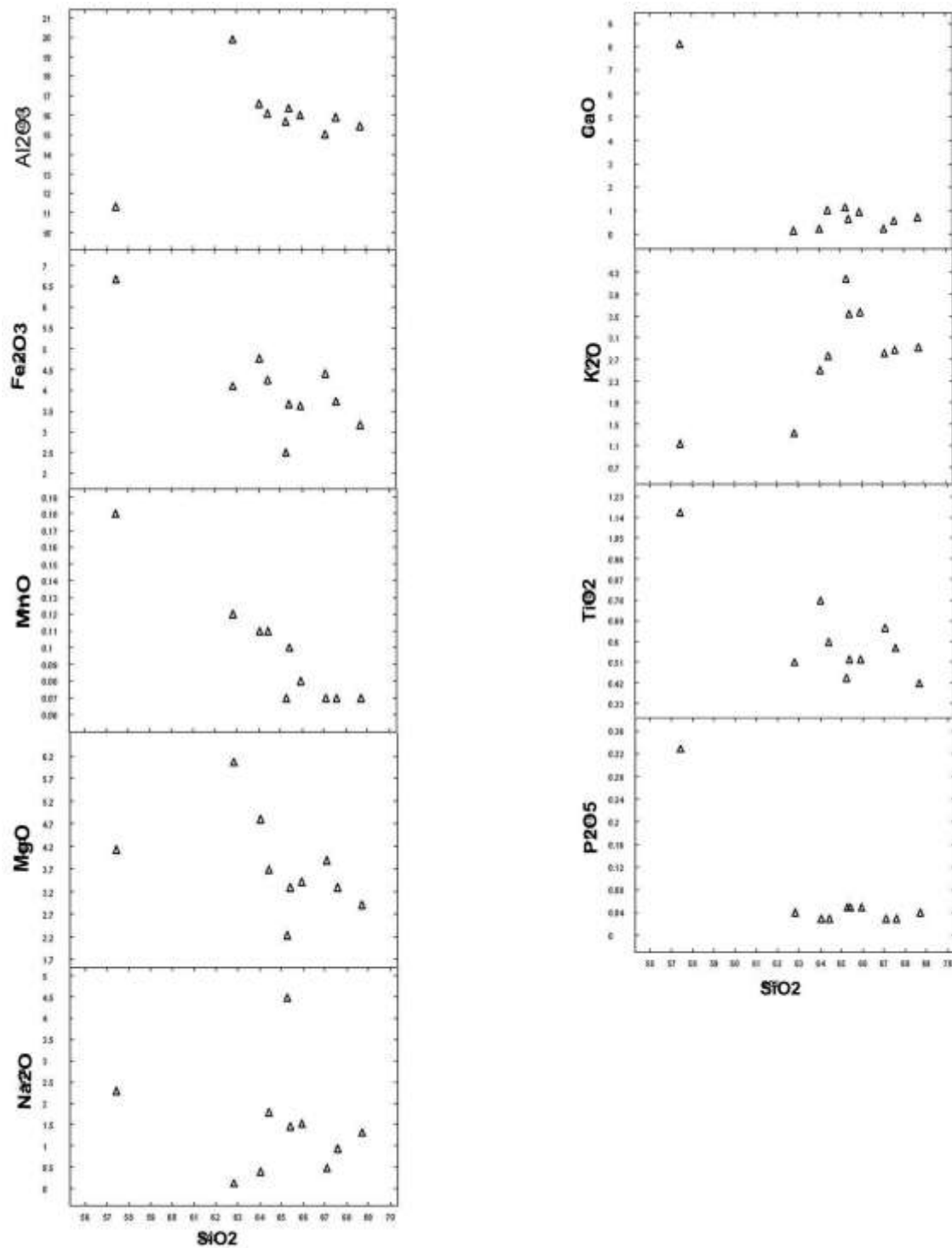


Figure 4. SiO₂ variation diagram for major oxides of metapelites of Sonapahar.

litic samples. However, La vs Th, Hf vs Zr, Ta vs Zr and Sr vs Ba (Fig. 5) shows a strong positive correlation. Strong positive correlation between Hf and Zr may reflect the influence of Zr on the budgets of Hf and follows the inheritance of compositional features from magmatic protolith. A value for Cu falls between (0.21-1.88 ppm) and values for Zn falls between 26.97-69.46 ppm except one sample with 13.63 ppm. The concentrations of gallium (18.09-32.04 ppm) are much higher than the crustal average ~ 17 ppm.⁷ Concentrations of Ba (156.25 -586.19 ppm) with average 447.13 ppm are quite lower than upper crustal average ~628 ppm. Cs concentrations are very low (4.86-11.26 ppm) (Table. 3). Concentrations of Cr and Ni are thought to be greater in Archean than in post Archean sediments.^{7,15-18} The concentrations of Cr (3.6-7.8 ppm) and Ni (1.4-3.8 ppm) in Sonapahar metapelites are distinctly low suggesting that ultramafic or (mafic) rocks were not important contributors

to their protolith.

The geodynamic environments in which the protoliths were formed was identified with the use of well known discriminant diagrams: Rb vs. Yb + Ta, Rb vs Y+Nb, Nb vs. Y, and Ta vs. Yb.^{19,20} In the tectonic-setting discrimination diagrams based on the Rb vs. (Yb + Ta), the composition of these rocks straddle the boundary regions between island-arc and syn collision granite field. In Nb vs. Y, Rb vs Y+Nb and Ta vs. Yb diagram, the composition plotted well within VAG to Syn-COLG field (Fig. 6).

Rare earth elements (REE)

The most informative parameters for REE and other trace elements are the sum of REE; the ratio of the sum of LREE to the sum of HREE $(LREE/HREE)_N$, which is interpreted as an indicator of paleoclimate; $(La/Yb)_N$, the slope of the REE pattern and some indicator

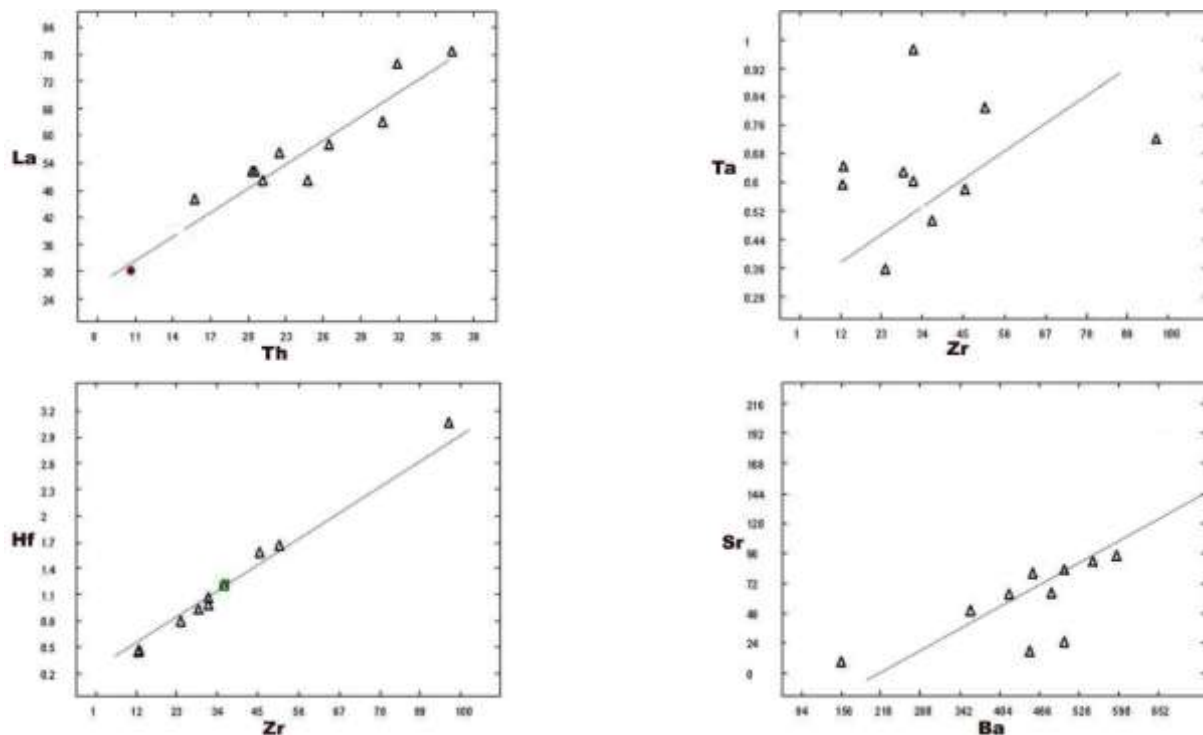


Figure 5. Variation diagram for La vs Th, Hf vs Zr, Ta vs Zr and Sr vs Ba of Sonapahar metapelites.

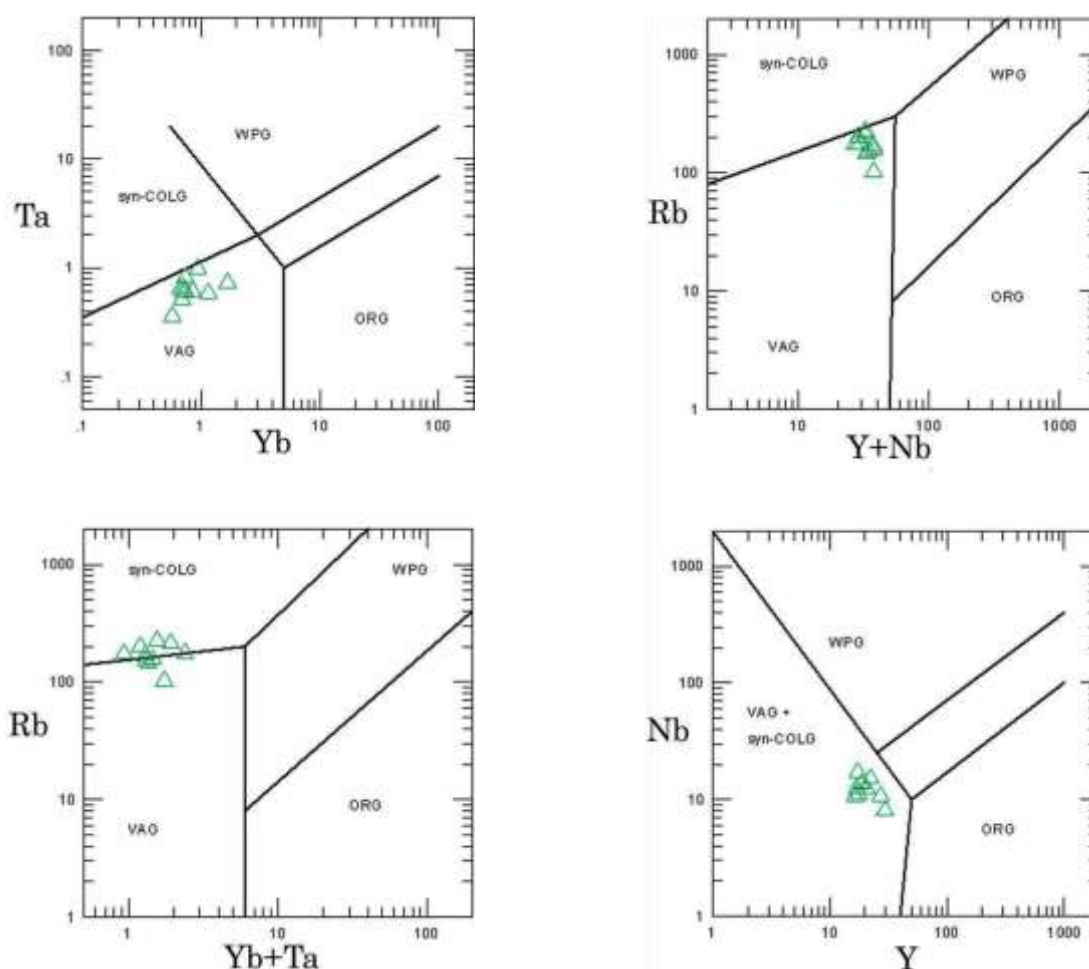


Figure 6. (a) Ta vs. Yb, (b) Rb vs. Y + Nb, (c) Rb vs. Yb + Ta and (d) Nb vs. Y discriminant diagrams for the metapelites of the Sonapahar area allowing reproducing the tectonic environments in which the granitoids were produced. Compositional fields of the granitoids: post-COLG–postcollision, syn-COLG–collision, VAG–island-arc, WPG–within-plate, ORG–oceanic ridges. The dashed lines in the Nb vs. Y and Ta vs. Yb diagrams mark the ORG boundary for normal rifts.

ratios of trace elements, such as La/Sc, Th/Sc, La/Th and Th/U. Chondrite normalize REE patterns²¹ of all the rock revealed overall enrichments of light rare earth elements (LREE) (Fig. 7) and fractionated LREE/HREE patterns. The REE pattern is characterized by prominent negative Eu-anomaly ($Eu/Eu^* = 0.17-0.68$). A significant negative slopes as follows from the relatively high val-

ues of $(La/Yb)_N = 16.67-68.98$. Despite the limited number of analysed samples, different levels of ΣREE have been observed. The ΣREE content in metapelites ranges from 204.11 ppm to 375.58 ppm.

Among the lithophile elements, the concentrations of Rb, Cs and Ba in the metapelites were slightly lower than PAAS. The marked trough at Sr probably suggests the fractiona-

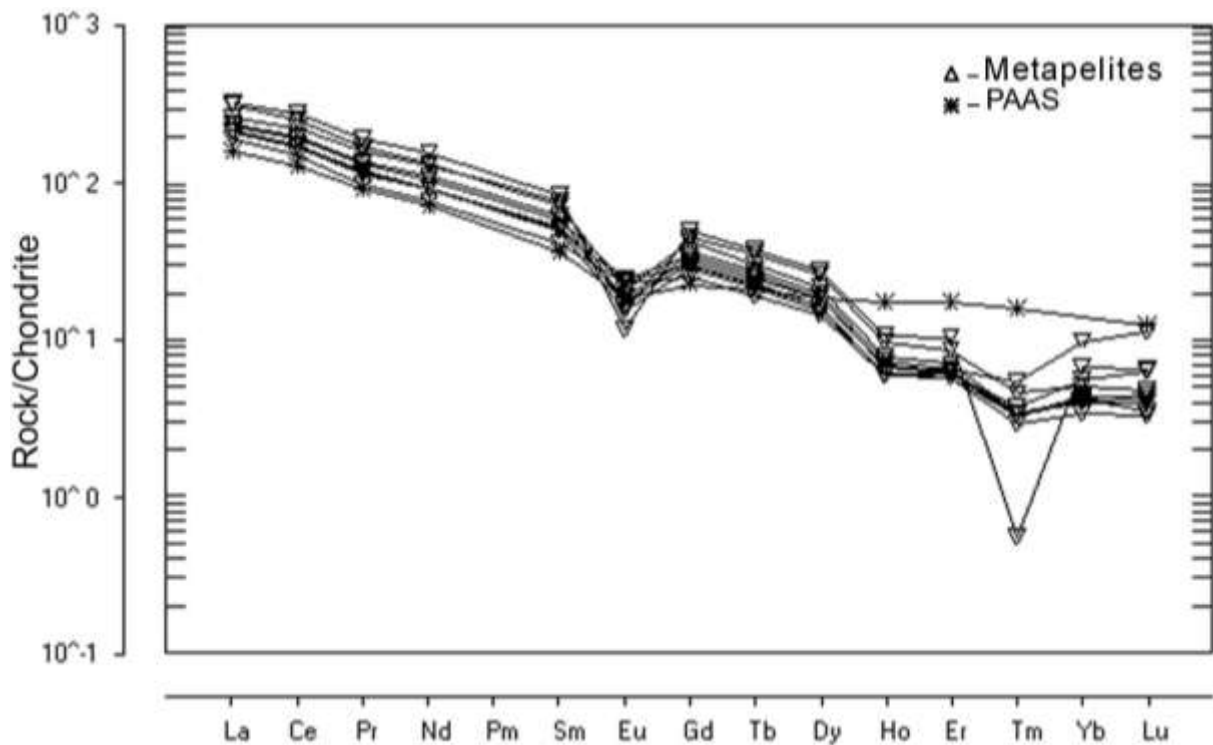


Figure 7. Concentration patterns of REE in metapelites normalized with the values of CI chondrite.

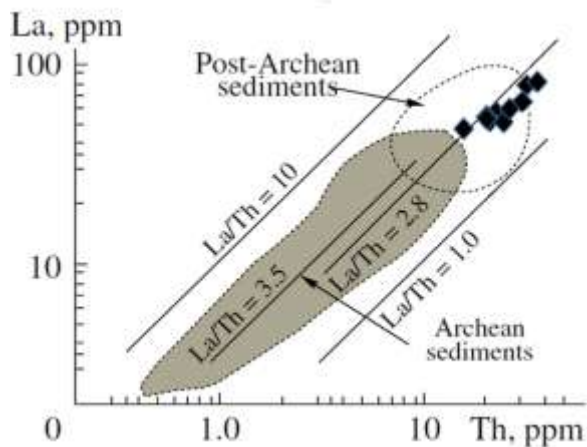


Figure 8. La vs. Th diagrams for the metapelites of Sonaphar.

tion of plagioclase feldspar during fractional crystallization of parent basalts. Among the high field strength elements (HFSE), Zr, Hf, and Ta were characterized by low concentration. However, U and Th roughly coincided with PAAS.

Thorium correlate strongly with the LREE in many sedimentary rocks.²² The La/Th ratio for most post-Archean sedimentary rocks from Australia is nearly constant at $\sim 2.7 \pm 0.2$ (at 95% confidence level).²³ In the present studied samples, Th correlate well with La (LREE) (Fig. 5) and the La/Th ratio range from 2.06-2.91. In La vs. Th diagram,²⁴ the data points of the metapelites were mostly constrained to the field of post-Archean cratonic deposits (Fig. 8). In addition, REE fractionated pattern and a pronounced negative Eu anomaly (Eu/Eu^* : 0.17-0.63), are well

within the compositional range of various post-Archaean shale estimates.⁷ It follows therefore that the Sonapahar metapelites were metamorphosed post-Archean sediments. The erosion of acid rocks was also evident from the elevated values of $Th/Sc = 2.6-3.4$ and $Th/U = 6.06-15.37$ relative to those PAAS. These rocks plotted within the compositional field of chlorite-rich clays in the MM vs. NAM diagram,¹⁴ where NAM is the modulus of normalized alkalinity equal to $(Na_2O + K_2O)/Al_2O_3$ (Fig. 9), which was used to classify clayey rocks. The high REE abundance ($\Sigma REE = 204.11-375.58$ ppm) in Sonapahar metapelites could be due to the abundance of accessory minerals. It has been suggested that the accessory minerals are considered as the main host of REE. In the REE patterns, metapelites were relatively depleted in HREE as compare to PAAS. This may be due to the presence of garnet and zircon in the source, for there is a large variation the partition coefficient of REE. This is consistent with the frequent occurrences of garnet and zircon halos in petrographic observations (Fig. 3).

CONCLUSION

The analysis of the newly obtained geochemical data on the distributions of major and trace elements, including REE, in these metapelites allowed us to reproduce the composition and nature of their protolith. Geochemically, the metapelites of the Sonapahar area were peraluminous with significant europium anomalies, fractionated REE pattern with enrichment of LREE. We determined that the rocks were redeposited and metamorphosed weathering crusts of the chlorite rich clay sediments and the eroded material coming to the sedimentation was more geochemically mature. The petro- and geochemical characteristics of the metapelites indicated that the protolith were formed of the erosion products of post-Archean rock complexes of predominantly acid (granitoid) composition. Our conclusions about the nature and compo-

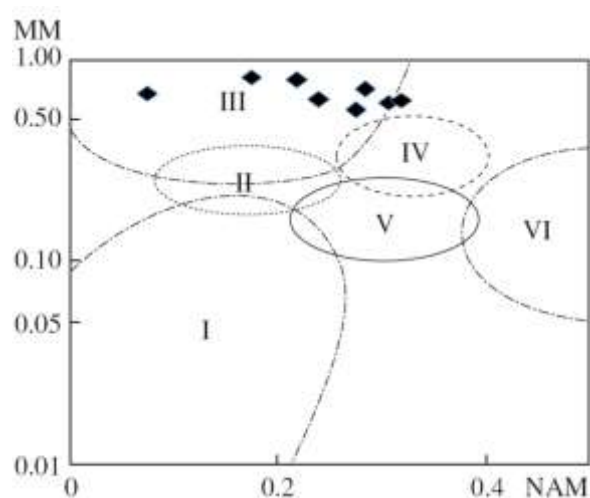


Figure 9. MM vs. NAM modulus diagram for the metapelites of the Sonapahar area. The MM axis is in a logarithmic scale. Compositional fields of clay rocks: (I) predominantly kaolinite clays; (II) montmorillonite-kaolinite-hydromica clays; (III) chlorite-rich clays with subordinate contents of Fe-hydromicas; (IV) chlorite-hydromica clays; (V) chlorite-montmorillonite clays; (VI) predominantly hydromica clays with feldspars.

sition of the protolith of these rocks are consistent with the results geodynamic reconstructions. The geochemical data suggested that the protolith of the metapelites were emplaced in volcanic arc granite to syn-collisional granitoid environment.

ACKNOWLEDGEMENT

Funding of this research project by UGC to the author is gratefully acknowledged. The authors are also thankful to the Department of Geology, Mizoram University, for providing facilities to carry out this work.

REFERENCES

1. Nandy DR & Das Gupta S (1986). Application of remote sensing in regional geological studies - a case study in

- northeastern part of India. In: *Proceedings of the International Seminar on Photogrammetry and Remote Sensing for Developing Countries*. Survey of India, New Delhi, pp. 4-6.
2. Bilham R & England P (2001). Plateau 'pop-up' in the great Assam Earthquake. *Nature*, 410, 806-809.
 3. Dasgupta S & Nandy DR (1982). Seismicity and tectonics of Meghalaya Plateau, North-eastern India. In: *Proceedings of the Symposium on Earthquake Engineering*. University of Roorkee, pp. 19-24.
 4. Chatterjee N, Mazumder AC, Battacharya A & Saikia RR (2007). Mesoproterozoic granulites of the Shillong - Meghalaya Plateau: Evidence of westward continuation of the Prydz Bay Pan- African suture into Northeastern India. *Precambrian Res*, 152, 1-26.
 5. Lal RK, Ackermant D, Seifert F & Haldar SK (1978). Chemographic relationships in sapphirine-bearing rocks from Sonapahar, Assam, India. *Contrib Mineral Petrol*, 67, 169-187.
 6. Cox R, Lowe DR & Cullers RL (1995). The influence of sediment recycling and basement composition on evolution of mudrock chemistry in the South Western United States. *Geochim Cosmochim Acta*, 59, 2919-2940.
 7. Taylor SR & McLennan SM (1985). *The Continental Crust: Its Composition and Evolution*. Blackwell Scientific Publications, Oxford, pp. 312.
 8. Chao TT & Sanzolone RF (1992). Decomposition techniques. *J Geochem Explor*, 44, 65-106.
 9. Roy P, Balaram V & Kumar A (2007). New REE and trace element data on two kimberlitic reference materials by ICP-MS. *Geostand Geoanal Res*, 31, 261-273.
 10. Symmes GH & Ferry JM (1992). Metamorphism, fluid flow and partial melting in pelitic rocks from the Onawa Contact Aureole, Central Maine, USA. *J Petrol*, 36, 587-612.
 11. Nesbitt HW & Young GM (1982). Early Proterozoic climates and plate motions inferred from major element chemistry of lullites. *Nature*, 299, 715-717.
 12. Harnois L (1988). The CIW index: a new chemical index of weathering. *Sediment Geol*, 55, 319-32.
 13. Fedo CM, Nesbitt HW & Young GM (1995). Unraveling the effects of potassium metasomatism in sedimentary rocks and paleosols, with implications for paleoweathering conditions and provenance. *Geology*, 23, 921-924.
 14. Likhanov II, Reverdatto VV & Vershinin AE (2008). Fe- and Al-rich metapelites of the Teiskaya Group, Yenisei Range: geochemistry, protoliths, and the behavior of their material during metamorphism. *Geochem Int*, 46, 17-36.
 15. Danchin RV (1967). Chromium and nickel in the Fig tree shales from South Africa. *Science*, 158, 261-262.
 16. Gibbs AK, Montgomery CW, O'Day PA & Erslev EA (1986). The Archean- Proterozoic transition: Evidence from the geochemistry of metasedimentary rocks of Guyana and Montana. *Geochim Cosmochim Acta*, 50, 2125-2142.
 17. Wronkiewicz DJ & Condie KC (1987). Geochemistry of Archean shales from the Witwatersrand Supergroup, South Africa: Source area weathering and provenances. *Geochim Cosmochim Acta*, 51, 2401-2416.
 18. McLennan SM & Taylor SR (1998). Crustal evolution: **Comments on the paper "The Archean- Proterozoic transition: Evidence from the geochemistry of metasedimentary rocks of Guyana and Montana" by Gibbs et al. (1986).** *Geochim Cosmochim Acta*, 52, 785-788.
 19. Pearce JA, Harris NBW & Tindle AG (1984). Trace element discrimination diagrams for the tectonic interpretation of granitic rocks. *J Petrol*, 25, 956-983.
 20. Pearce JA (1996). Sources and settings of granitic rocks. *Episodes*, 19, 120-125.
 21. Sun SS, Mc Donough WF, (1989). Chemical and isotopic systematic of oceanic basalts: implication for mantle composition and processes. In: *Magmatism in the Ocean Basins* (AD Saunders & MJ Norry, eds). *Spec Publ-Geol Soc London*, 42, 313-34.
 22. Mc Lennan SM, Lance WB & Taylor SR (1980). Rare Earth Element - Thorium correlation in sedimentary rocks, and the composition of continental crust. *Geochim Cosmochim Acta*, 44, 1833-1839.
 23. McLennan SM (1982). On the geochemical evolution of sedimentary rocks. *Chem Geol*, 37, 335-350.
 24. McLennan SM (1989). Rare earth elements in sedimentary rocks: influence of provenance and sedimentary processes. *Geochem Mineral Rare Earth Elem*, 21, 169-200.
 25. Mazumder SK (1976). A summary of the Precambrian geology of the Khasi Hills, Meghalaya. *Geol Surv India Misc Publ*, 23, 311-324.